
Towards Global Optimality in Cooperative MARL with Sequential Transformation

Jianing Ye

Tsinghua University
yejn21@mails.tsinghua.edu.cn

Chenghao Li

Tsinghua University
lich18@mails.tsinghua.edu.cn

Jianhao Wang

Tsinghua University
wjh19@mails.tsinghua.edu.cn

Chongjie Zhang

Tsinghua University
chongjie@tsinghua.edu.cn

Abstract

Policy learning in multi-agent reinforcement learning (MARL) is challenging due to the exponential growth of joint state-action space with respect to the number of agents. To achieve higher scalability, the paradigm of centralized training with decentralized execution (CTDE) is broadly adopted with factorized structure in MARL. However, we observe that existing CTDE algorithms in cooperative MARL cannot achieve optimality even in simple matrix games. To understand this phenomenon, we introduce a framework of Generalized Multi-Agent Actor-Critic with Policy Factorization (GPF-MAC), which characterizes the learning of factorized joint policies, i.e., each agent's policy only depends on its own observation-action history. We show that most popular CTDE MARL algorithms are special instances of GPF-MAC and may be stuck in a suboptimal joint policy. To address this issue, we present a novel transformation framework that reformulates a multi-agent MDP as a special "single-agent" MDP with a sequential structure and can allow employing off-the-shelf single-agent reinforcement learning (SARL) algorithms to efficiently learn corresponding multi-agent tasks. This transformation retains the optimality guarantee of SARL algorithms into cooperative MARL. To instantiate this transformation framework, we propose a Transformed PPO, called T-PPO, which can theoretically perform optimal policy learning in the finite multi-agent MDPs and shows significant outperformance on a large set of cooperative multi-agent tasks.

1 Introduction

Cooperative multi-agent reinforcement learning (MARL) is a promising approach to a variety of real-world applications, such as sensor networks [Zhang and Lesser, 2011], traffic light control [Van der Pol and Oliehoek, 2016], and multi-robot formation [Alonso-Mora et al., 2017]. However, "the curse of dimensionality" is one major challenge in cooperative MARL, since the joint state-action space grows exponentially with respect to the number of agents. To achieve higher scalability, factorized structures are employed within the paradigm of centralized training with decentralized execution (CTDE) [Kraemer and Banerjee, 2016a], which allows agents to learn their local policies in a centralized way while retaining the ability of decentralized execution.

Recently, many factorized MARL algorithms have been proposed. For value-based methods, the joint Q value is factorized as a function of individual Q values of agents. To enable scalability and decentralized execution, it is critical to ensure the joint greedy action can be computed by selecting local greedy actions through individual Q functions, which is formalized as the Individual-Global-

Max (IGM) principle [Son et al., 2019]. Based on this IGM property, a series of factorized multi-agent Q-learning methods have been developed, including but not limited to VDN [Sunehag et al., 2018], QMIX [Rashid et al., 2018], QTRAN [Son et al., 2019] and QPLEX [Wang et al., 2021b]. For multi-agent actor-critic methods, the joint policy is often factorized into the direct product of individual policies, each of which is learned through policy gradient updates. For example, COMA [Foerster et al., 2018] and DOP [Wang et al., 2021c] aim at the critic design for effective credit assignment, MADDPG [Lowe et al., 2017] studies the situation with parameterized deterministic policies, and MAPPO [Yu et al., 2021] applies PPO to multi-agent settings with parameter sharing.

Despite promising performance in benchmark tasks, these factorized MARL methods do not have a global optimality guarantee in general cooperative settings and may fail to achieve optimality even in simple matrix games. To understand this phenomenon, we introduce a general framework, called Generalized Multi-Agent Actor-Critic with Policy Factorization (GPF-MAC), to characterize both value-based and actor-critic MARL methods with factorized structure. We show that GPF-MAC that aims to optimize the expected value objective may converge to a suboptimal factorized joint policy. To address this suboptimality issue, we present a novel transformation framework that reformulates a multi-agent MDP as a special “single-agent” MDP with a sequential decision-making structure among agents. This transformation allows off-the-shelf single-agent reinforcement learning (SARL) methods to efficiently learn coordination policies in cooperative multi-agent tasks and retain their global optimality guarantee. To instantiate this transformation framework, we propose a Transformed PPO (T-PPO), which can theoretically perform optimal policy learning in finite-multi-agent MDPs and empirically shows significant outperformance on a large set of cooperative multi-agent tasks.

2 Preliminaries & Related Work

2.1 RL Models

In single-agent RL (SARL), an agent interacts with a Markov Decision Process (MDP) to maximize its cumulative reward [Sutton and Barto, 2018]. An MDP is defined as a tuple $(\mathcal{S}, \mathcal{A}, r, P, \gamma, s_0)$, where \mathcal{S} and \mathcal{A} denote the state space and action space. At each time step t , the agent observes the state s_t , and chooses an action $a_t \in \mathcal{A}$, where $a_t \sim \pi(s_t)$ depends on s_t and its policy π . After that, the agent will gain an instant reward $r_t = r(s_t, a_t)$, and transit to the next state $s_{t+1} \sim P(\cdot|s_t, a_t)$. γ is the discount factor. The goal of an SARL agent is to optimize a policy π that maximizes the expected cumulative reward, i.e., $\mathcal{J}(\pi) = \mathbb{E}_{s_{t+1} \sim P(\cdot|s_t, \pi(s_t))} [\sum_{t=0}^{\infty} \gamma^t r(s_t, \pi(s_t))]$.

In MARL, we model a fully cooperative multi-agent task as a Dec-POMDP [Oliehoek et al., 2016] defined by a tuple $(\mathcal{N}, \mathcal{S}, \mathcal{A}, P, \Omega, O, r, \gamma)$, where \mathcal{N} is a set of agents and \mathcal{S} is the global state space, \mathcal{A} is the action space, and γ is a discount factor. At each time step, agent $i \in \mathcal{N}$ has access to the observation $o_i \in \Omega$, drawn from the observation function $O(s, i)$. Each agent has an action-observation history $\tau_i \in \Omega \times (\mathcal{A} \times \Omega)^*$ and constructs its individual policy $\pi(a_i|\tau_i)$. With each agent i selecting an action $a_i \in \mathcal{A}$, the joint action $\mathbf{a} \equiv [a_i]_{i=1}^n$ leads to a shared reward $r = R(s, \mathbf{a})$ and the next state s' according to the transition distribution $P(s'|s, \mathbf{a})$. The formal objective of MARL agents is to find a joint policy $\boldsymbol{\pi} = \langle \pi_1, \dots, \pi_n \rangle$ conditioned on the joint trajectories $\boldsymbol{\tau} \equiv [\tau_i]_{i=1}^n$ that maximizes a joint value function $V^{\boldsymbol{\pi}}(s) = \mathbb{E}[\sum_{t=0}^{\infty} \gamma^t r_t | s_0 = s, \boldsymbol{\pi}]$. Another quantity in policy search is the joint action-value function $Q^{\boldsymbol{\pi}}(s, \mathbf{a}) = r(s, \mathbf{a}) + \gamma \mathbb{E}_{s'}[V^{\boldsymbol{\pi}}(s')]$.

To simplify our analysis, we present a framework of Multi-agent MDPs (MMDP) [Boutillier, 1996], a special case of Dec-POMDP, to model cooperative multi-agent decision-making tasks with full observations. MMDP is defined as a tuple $(\mathcal{N}, \mathcal{S}, \mathcal{A}, P, r, \gamma)$, where \mathcal{N} , \mathcal{S} , \mathcal{A} , P , r , and γ are the same agent set, state space, action space, transition function, reward function, and discount factor in Dec-POMDP, respectively. Due to the full observations, at each time step, the current state s is observable to each agent. For each agent i , a individual policy $\hat{\pi}_i(a|s)$ represents a distribution over actions conditioned on the state s . Agents aim to find a joint policy $\hat{\boldsymbol{\pi}} = \langle \hat{\pi}_1, \dots, \hat{\pi}_n \rangle$ that maximizes a joint value function $\hat{V}^{\hat{\boldsymbol{\pi}}}(s)$, where denoting $\hat{V}^{\hat{\boldsymbol{\pi}}}(s) = \mathbb{E}[\sum_{t=0}^{\infty} \gamma^t r_t | s_0 = s, \hat{\boldsymbol{\pi}}]$.

2.2 Policy Factorization and Centralized Training with Decentralized Execution

In MARL, due to partial observability and communication constraints, each agent needs to make its own decision based on its local action-observation history during execution, i.e., the joint execution policy $\boldsymbol{\pi}^{test}$ can be decomposed into a product of individual execution policies $[\pi_i^{test}]_{i=1}^n$, called

policy factorization: $\forall \tau$,

$$\pi^{test}(\mathbf{a}|\tau) = \prod_{i=1}^n \pi_i^{test}(a_i|\tau_i). \quad (1)$$

In order to effectively learn π^{test} , centralized training with decentralized execution (CTDE) becomes a popular paradigm of cooperative MARL Oliehoek et al. [2008], Kraemer and Banerjee [2016b]. In CTDE, agents are trained in a centralized manner and are granted access to other agents' information or global state during the centralized training process. Denote the joint policy π^{train} which is learned during training. Note that during centralized training, the constraint of policy factorization (see Eq. 1) is not necessary for π^{train} and the agents can use joint policy π^{train} to interact with the environments for collecting training data. However, most popular CTDE MARL algorithms [Foerster et al., 2018, Lowe et al., 2017, Wang et al., 2021c, Yu et al., 2021, de Witt et al., 2020, Sunehag et al., 2018, Rashid et al., 2018, Son et al., 2019, Wang et al., 2021b] encode the policy factorization defined in Eq. (1) into the training joint policy π^{train} and these algorithms can be divided into two categories: actor-critic and value-based.

For recent actor-critic algorithms [Foerster et al., 2018, Lowe et al., 2017, Wang et al., 2021c, Yu et al., 2021, de Witt et al., 2020], a joint (stochastic or deterministic) policy can be represented as product of individual policies, i.e., $\pi(\mathbf{a}|\tau) = \prod_{i=1}^N \pi_i(a_i|\tau_i)$, which corresponds to policy factorization defined in Eq. (1).

For value-based algorithms [Sunehag et al., 2018, Rashid et al., 2018, Son et al., 2019, Wang et al., 2021b], IGM (*Individual-Global-Max*) [Son et al., 2019] is a popular principle to realize effective value-based CTDE, which asserts the consistency between joint and local greedy action selections in the joint action-value $Q_{tot}(\tau, \mathbf{a})$ and local action-values $[Q_i(\tau_i, a_i)]_{i=1}^n$, respectively: $\forall \tau$,

$$\arg \max_{\mathbf{a} \in \mathcal{A}} Q_{tot}(\tau, \mathbf{a}) = \left\langle \arg \max_{a_1 \in \mathcal{A}} Q_1(\tau_1, a_1), \dots, \arg \max_{a_n \in \mathcal{A}} Q_n(\tau_n, a_n) \right\rangle. \quad (2)$$

Denote the greedy joint policy $\pi(\mathbf{a}|\tau) = \arg \max_{\mathbf{a} \in \mathcal{A}} Q_{tot}(\tau, \mathbf{a})$ and the greedy individual policies $\pi_i(a_i|\tau_i) = \arg \max_{a_i \in \mathcal{A}} Q_i(\tau_i, a_i)$. We have $\pi(\mathbf{a}|\tau) = \prod_{i=1}^N \pi_i(a_i|\tau_i)$, which is called policy factorization defined in Eq. (1). Although various value factorizations [Wang et al., 2021a] are widely studied in the literature, to our best knowledge, this paper is the first to study the effect of policy factorization in the perspective of optimality policy learning.

3 Motivation: Suboptimality of MARL with Factorized Structures

In this section, we will formally analyze the potential suboptimality of cooperative MARL with a factorized joint policy. We will first describe a general MARL framework, called Generalized Multi-Agent Actor-Critic with Policy Factorization (GPF-MAC), which generalizes both actor-critic and value-based methods of cooperative MARL for learning a factorized joint policy. We then show that multi-agent actor-critic methods with policy factorization may get stuck in suboptimal policies and defer the suboptimality analysis of factorized value-based cooperative MARL methods to Appendix A.2.

Here we formalize a class GPF-MAC of multi-agent algorithms in order to simplify the analysis of empirical algorithms with factorized policy.

Definition 3.1. *Generalized Multi-agent Actor-Critic with Policy Factorization (GPF-MAC)*

An algorithm is called to be in GPF-MAC, if it contains three parts:

- *The factorized joint policy (can be deterministic or stochastic): $\pi_{\Theta} = \pi_{\theta_1} \times \dots \times \pi_{\theta_n}$, where n is the number of agents, θ_i is the parameters of the individual policy of agent i , and $\Theta = \bigcup_{i=1}^n \theta_i$ are agents' joint policy parameters. For value-based methods, θ_i can be the parameters of the Q -value network of agent i , which implicitly represent its local policy. Based on our definition, parameter sharing is allowed among agents.*
- *The loss function $C(\theta_1, \dots, \theta_n)$ is the optimization objective, which can be the TD loss for value-based methods and the negative of the expected value of the joint policy for actor-critic methods.*

- The optimization method \mathcal{E} : \mathcal{E} is used to minimize $C(\theta_1, \dots, \theta_n)$ with respect to the policy parameters. In this paper, we assume \mathcal{E} to be some variant of the gradient descent method.

and its learning process is conducted as in Algorithm 1.

Algorithm 1 Generalized Multi-Agent Actor-Critic with Factorization

Initialization: Policy parameters Θ .
while iteration not finished **do**
 The parameter update direction \mathbf{g} is calculated by $\mathcal{E}(C, \Theta)$ to approximate $\nabla_{\Theta} C(\theta_1, \dots, \theta_n)$.
 Update the factorized joint policy by \mathbf{g} : $\Theta \leftarrow \Theta - \alpha * \mathbf{g}$
end while
return The factorized joint policy $\pi_{\Theta} = \pi_{\theta_1} \times \dots \times \pi_{\theta_n}$.

It is straightforward to show that most existing MARL methods with factorized policy are instances of GPF-MAC, including actor-critic methods, such as MAPPO, COMA, MADDPG, and DOP, and value-based methods such as VDN, QMIX, QTRAN, and QPLEX.

To analyze the suboptimality of GPF-MAC, we focus on the local minimums of C , since \mathcal{E} is some variant of gradient descent method to optimize C , which is prone to get stuck in local optimums.

For different MARL methods, the characteristic of a local minimum can be different. For actor-critic instances of GPF-MAC, i.e. GPF-MACs with loss function $C(\theta_1, \dots, \theta_n) = -J(\pi_{\Theta})$, the negative of the expected value of the joint policy, its local (or global) minimum is corresponding to the local (or global) optimal joint policy. For some cooperative tasks, there exist multiple Nash equilibria, some of which are suboptimal. In these tasks, actor-critic algorithms naturally tend to lose their global optimality guarantee.

For example, considering the following matrix game (Table 1). The row player selects an index r of rows ($r \in \{0, 1, 2\}$), and the column player selects an index c of columns ($c \in \{0, 1, 2\}$). Then $(0, 0)$, $(1, 1)$, $(2, 2)$ are three different Nash's Equilibria of this matrix game with different payoff 10, 5, 1. Only $(0, 0)$ is the global optimal policy. However, policy $(1, 1)$ and $(2, 2)$ will have zero policy gradient, no matter what parameterization of local policies are due to Proposition 3.1.

10	-20	-20
-20	5	0
-20	0	1

Table 1: Matrix Game with multiple Nash Equilibria

Proposition 3.1. *For the actor-critic instance of GPF-MAC optimized by gradient descent, any Nash's Equilibrium of policies is a stationary point.*

Proof is presented in Appendix A.2.

In contrast, for value-based MARL methods, the loss function $C(\theta_1, \dots, \theta_n)$ is the TD loss, and its local (or global) minimum is not necessarily corresponding to the local (or global) optimal joint policy. Thus, the analysis of these algorithms need to take closer look to their loss function C and optimization method \mathcal{E} , and analyze them one by one, which are deferred to Appendix A.2.

4 A Sequential Transformation Framework for MARL Problems

To achieve global optimality in cooperative MARL, we propose a novel transformation framework that can reformulates a Multi-agent MDP (MMDP) as a special "single-agent" MDP with a sequential structure. This MDP transformation naturally provides a corresponding policy transformation, in which the policies in the MMDP and MDP can be converted to each other. In particular, the optimal policy in MDP can be converted to the optimal policy in the original MMDP. These MDP and policy transformation allow us to employ any single-agent RL (SARL) algorithm to efficiently learn corresponding multi-agent tasks. From the optimality guarantee of SARL algorithm, we can achieve the global optimality in the challenging MARL tasks. In the theoretical perspective, we also find that this transformation keep the same sample complexity. To instantiate this transformation framework,

we propose a Transformed PPO, called T-PPO, which incorporates the remarkable empirical ability of PPO [Schulman et al., 2017b] and theoretical optimality guarantee in the finite MMDPs.

4.1 Sequential Transformation

We define the sequential transformation as follows.

Definition 4.1 (Sequential Transformation Γ). *Given an MMDP $\mathcal{M} = (\mathcal{S}, \mathcal{A}, P, r, \gamma, s_0, N)$, its sequential transformation is an MDP $\Gamma(\mathcal{M}) = (\tilde{\mathcal{S}}, \mathcal{A}, \tilde{P}, \tilde{r}, \tilde{\gamma}, s_0)$, where $\tilde{\mathcal{S}} = \bigcup_{i=0}^{N-1} \mathcal{S} \times \mathcal{A}^i$ is the state space, \mathcal{A} is the same action space as the original MMDP \mathcal{M} , \tilde{P} is the transformed transition function, where $\forall k < N, \forall \tilde{s} = (s, a_1, \dots, a_{k-1}) \in \tilde{\mathcal{S}}, \forall a_k \in \mathcal{A}$, we have $\tilde{P}((s, a_1, \dots, a_k) | \tilde{s}, a_k) = 1$, and $\forall \tilde{s} = (s, a_1, \dots, a_{N-1}) \in \tilde{\mathcal{S}}, \forall s' \in \mathcal{S}, \forall a_N \in \mathcal{A}$, we have $\tilde{P}(s' | \tilde{s}, a_N) = P(s' | s, (a_1, \dots, a_N))$, \tilde{r} is the transformed reward function, where $\forall k < N, \forall \tilde{s} = (s, a_1, \dots, a_{k-1}) \in \tilde{\mathcal{S}}, \forall a_k \in \mathcal{A}$, we have $\tilde{r}(\tilde{s}, a_k) = 0$, and $\forall \tilde{s} = (s, a_1, \dots, a_{N-1}) \in \tilde{\mathcal{S}}, \forall a_N \in \mathcal{A}$, we have $\tilde{r}(\tilde{s}, a_N) = r(s, (a_1, \dots, a_N))$, $\tilde{\gamma} = \gamma^{1/N}$ is a transformed discount factor, and s_0 is the initial state.*

It's easy to see that, $\Gamma(\mathcal{M})$ is the "sequential decision-making" version of \mathcal{M} . That is, agent $1, \dots, N$ take actions sequentially. Previously selected actions are passed to later agents for their information.

In this way, if we have an MDP-policy $\Gamma(\mathcal{M})$, we can convert it to an MMDP-policy on \mathcal{M} in the way stated in Theorem 4.1:

Theorem 4.1. *For any deterministic policy π on $\Gamma(\mathcal{M})$, there is a decentralized policy $\pi_{jt} = (\pi_1, \dots, \pi_N)$ on \mathcal{M} such that $\mathcal{J}_{\mathcal{M}}(\pi_{jt}) = \gamma^{(1-n)/n} \mathcal{J}_{\Gamma(\mathcal{M})}(\pi)$, where $\pi_1(s) = \pi(s)$, $\pi_k(s) = \pi((s, \pi_1(s), \dots, \pi_{k-1}(s)))$ for all $k > 1$.*

For any stochastic policy η on $\Gamma(\mathcal{M})$, there is a communicated policy $\eta_{jt} = (\eta_1, \dots, \eta_N)$ on \mathcal{M} such that $\mathcal{J}_{\mathcal{M}}(\eta_{jt}) = \gamma^{(1-n)/n} \mathcal{J}_{\Gamma(\mathcal{M})}(\eta)$, where $\eta_1(a_1 | s) = \eta(a_1 | s)$, $\eta_k(a_k | s, a_1, \dots, a_{k-1}) = \eta(a_k | (s, a_1, \dots, a_{k-1}))$ for all $k > 1$, where a_1, \dots, a_{k-1} are actions selected by agents $1, \dots, k-1$.

And conversely, for any policy π_{jt} on \mathcal{M} , there is a policy π on $\Gamma\mathcal{M}$ such that $\mathcal{J}_{\mathcal{M}}(\pi_{jt}) = \gamma^{(1-n)/n} \mathcal{J}_{\Gamma(\mathcal{M})}(\pi)$.

The proof is presented in Appendix A.3.2.

Note that usually we can only access to an interactive environment of \mathcal{M} . So we need to wrap the interface to make the algorithm A run as if it's accessing to the interactive environment of $\Gamma(\mathcal{M})$. The whole sequential framework is described in pseudo-code in appendix (Algorithm 2).

Now we can claim the following corollary.

Corollary 4.1. *Using the sequential framework, if the SARL algorithm \mathfrak{A} is guaranteed to obtain an optimal policy on MDP, then the MARL algorithm $T\mathfrak{A}$ is guaranteed to obtain an optimal policy on MMDP.*

Thanks to the theoretical analysis for global optimality of PPO with neural network ([Liu et al., 2019]), we are able to claim a suitable implementation of T-PPO attains global optimality under the same mild assumptions in [Liu et al., 2019].

Corollary 4.2. *A suitable implementation of T-PPO converges to global optimum, if Assumption 4.1, 4.2, 4.3 in [Liu et al., 2019] holds, in particular, if \mathcal{M} is tabular.*

Corollary 4.2 is guaranteed directly by Theorem 4.9 in [Liu et al., 2019] and Corollary 4.1.

4.2 The Complexity of the Transformed Model

By sequential transform, we are able to convert any MMDP to an MDP and run SARL algorithms on the MDP to solve the MMDP. One natural question is, will such framework bring additional hardness of the task?

First of all, this framework obviously doesn't increase the minimax sample complexity of the task, since the MMDP \mathcal{M} and the MDP $\Gamma(\mathcal{M})$ can be transformed to each other with merely negligible

additional cost in time and space (see appendix A.5). Nevertheless, for a concrete algorithm A (e.g. Q-learning), the sample complexity is not necessary to be the same after such transformation.

Let’s take Q-learning as an example. We first investigate the size of state-action space before and after the transformation. It easy to see that the size of the state-action space of \mathcal{M} is $|\mathcal{S}||\mathcal{A}|^N$, and that of its $\Gamma(\mathcal{M})$ is $|\mathcal{A}| \sum_{i=0}^{N-1} |\mathcal{S}||\mathcal{A}|^i = |\mathcal{S}||\mathcal{A}| \frac{1-|\mathcal{A}|^N}{1-|\mathcal{A}|} \leq 2|\mathcal{S}||\mathcal{A}|^N$. This implies that the sequential transform does not increase the complexity in the state-action space.

However, if we take a closer look here of the sample complexity, we will find that the exact sample complexity bound of Q-learning is $O^* \left(\frac{|\mathcal{S}||\mathcal{A}|}{(1-\gamma)^4 \epsilon^2} \right)$ ([Li et al., 2021b]), which depends on not only the size of state-action space, but also on the magnitude of $\frac{1}{1-\gamma}$. This implies that the sample complexity may increase for certain algorithms since $\Gamma(\mathcal{M})$ has a longer horizon. Despite this unpleasant result, for Q-learning, still, this analysis leave out the structure of $\Gamma(\mathcal{M})$: for every n steps in $\Gamma(\mathcal{M})$ there are $n-1$ deterministic transitions with reward 0. So fortunately, if we modify the original Q-learning a little bit, it will attain the same sample complexity as before (See Appendix A.4).

4.3 T-PPO: Extension to Dec-POMDP

In practice, many MARL benchmarks are partially observable. To apply our algorithms to partial-observable environments, we need to extend our algorithms to Dec-POMDP. To instantiate our transformation framework, we propose a Transformed PPO (T-PPO) based on PPO [Schulman et al., 2017a]. The Actor-Critic structure is shown in Figure 1. Following the idea of sequential transformation discussed in Section 4.1, we introduce previous agents’ actions to each agent’s actor and critic modules. However, this sequential transformed information increases with respect to the number of agents. To achieve scalability, we additionally equip each agent’s actor and critic with a multi-head attention (MHA) module.

Intuitively, we believe considering too much information from previous agents’ actions is harmful to learning. So we add regularization terms to agents’ actor and critic modules respectively for encouraging each agent to extract critical information. As demonstrated by yellow modules in actor, policies $\pi_{i,T}^{(t)}$ used for training is combined with two parts: one part contains previous agents’ actions as inputs for the MHA module, and the other part only takes own trajectory as inputs ($\pi_{i,main}^{(t)}$). For regularization, we add KL divergence between $\pi_{i,main}^{(t)}$ and $\pi_{i,T}^{(t)}$ to decrease the influence of previous agents’ actions. A similar structure is also implemented in the critic structure as shown on the right side of Figure 1 with L1 norm for regularization. To enable decentralized execution, we further distill the communicated policy $\pi_{i,T}^{(t)}$ to a decentralized policy $\pi_{i,E}^{(t)}$ with behaviour cloning by optimising the cross entropy loss independently for each agent (see appendix B.2.3 for detail). Here we share GRU and the representation layer, whose inputs do not contain other agents’ information.

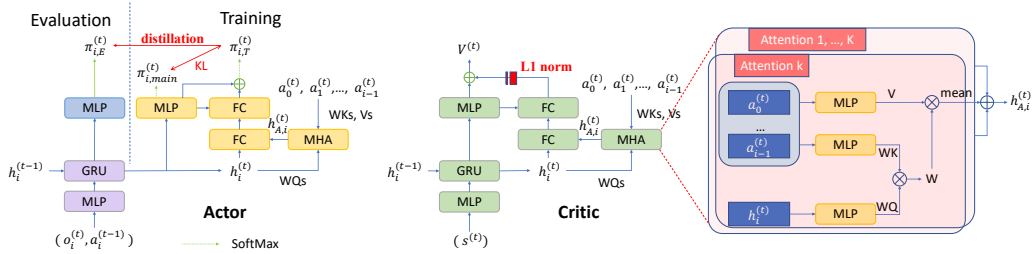


Figure 1: The architecture of combining our sequential transformation framework with PPO (T-PPO)

5 Experiments

We design experiments to answer the following questions: (1) Can the proposed sequential framework achieve the global optimal policy on MMDP? (Section 5.1 and Section 5.2.1) (2) Can our approach

improve learning efficiency for policy-based MARL algorithms? (Section 5.2 and Section 5.3) (3) Will distillation influence performance during decentralized execution? (Section 5.2 and Section 5.3)

We first use a multi-task matrix game to demonstrate the global optimality of our communicated policy compared to multi-agent value-based methods (VDN, QMIX, QTRAN, QPLEX), and policy-based methods (MAPPO, HAPPO[Kuba et al., 2021]). Then, we use challenging tasks from the StarCraft II micromanagement (SMAC) benchmark[Samvelyan et al., 2019] and Google Research Football (GRF) benchmark [Kurach et al., 2019] to further demonstrate and illustrate the outperformance of our approach. In each environment, We show the average and variance of the performance for our method and baselines tested with three random seeds (seed 0, 1, 2). For all baselines, we use the codes provided by the authors properly with the same hyper-parameters as the original papers.

5.1 Multi-task Matrix Game

To show that previous MARL algorithms cannot guarantee optimality, we introduce a multi-task matrix game here, which is a simple 1-step game with 2 players and 10 matrices (see Appendix B.1.1 for details).

We demonstrate the sum reward of all matrices for our approach and baselines in Figure 2. Our communicated policy converges to 100 immediately, demonstrating the global optimality of our sequential transformation framework. Other baseline algorithms get stuck in locally optimal solutions, which confirms the theorems we discussed above. Value-based methods VDN, QMIX, and QPLEX converge to a similar local optimal point at the end of training. Taking benefit from the duplex dueling network architecture, QPLEX has a stronger representative ability than VDN and QMIX. Nevertheless, such a complex structure creates a large number of local optimums at the agent level (see appendix A.2). QTRAN achieves convincing performance in some simple matrix games with an carefully designed regularizer tackling IGM. However, its discontinuous loss function will still hinder the global optimal solution. HAPPO and MAPPO get stuck in Nash’s Equilibrium due to proposition 3.1, and cannot guarantee global optimality. In this way, our approach dominates in our multi-task matrix game.

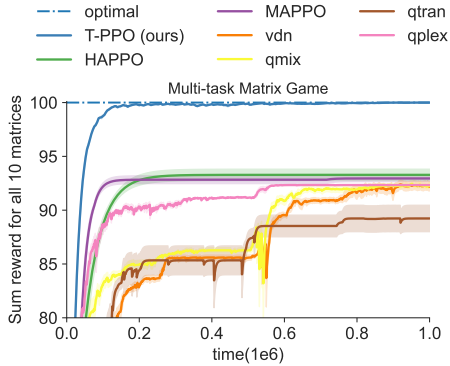


Figure 2: Learning curve of Multi-task Matrix Game

5.2 StarCraft II

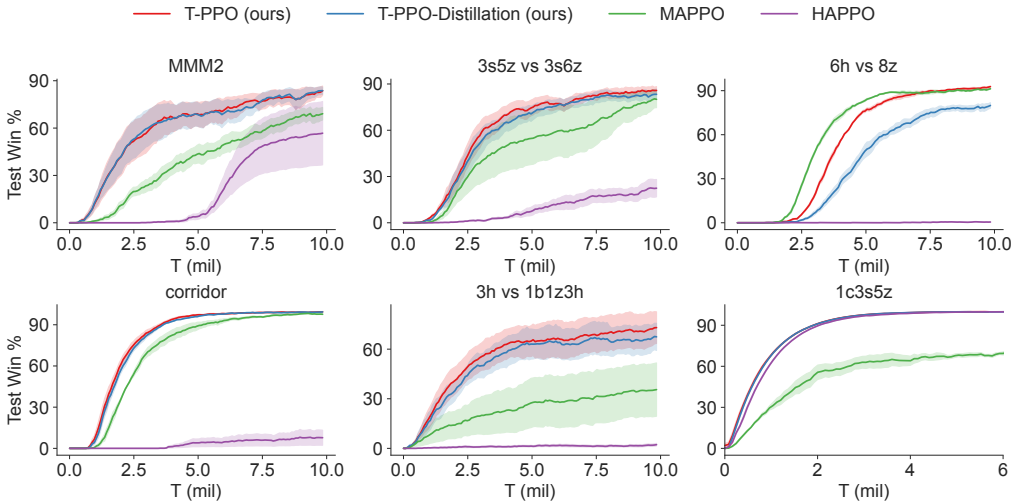


Figure 3: Learning curve of SMAC

The above multi-task matrix game demonstrates the global optimality of our sequential transformation framework. Here we further compare our approach with policy-based baselines on four super hard maps (MMM2, 3s5z_vs_3s6z, 6h_vs_8z, corridor), one easy map (1c3s5z), and one our own map (3h_vs_1b1z3h) based on the SMAC benchmark.

We illustrate the learning curve of StarCraft II in Figure 3. Our communicated policy outperforms baselines on five out of six maps while performing similarly with MAPPO on 6h_vs_8z. Super hard maps are typically hard-exploration tasks. However, taking benefits of our approach’s global optimality guarantee for MMDP, T-PPO can exploit better with the same exploration strategy as MAPPO (based on the entropy of learned policies). We will highlight a map 1c3s5z, where MAPPO converges to a locally optimal point but our approach achieves global optimality with nearly 100% winning rate. This phenomenon once again demonstrates the advantage of our sequential transformation framework. HAPPO can also achieve nearly 100% winning rate on 1c3s5z but fails on other maps. We believe it is still because local optimality of Nash equilibrium learned by HAPPO. Meanwhile, compared with our approach and MAPPO, agents cannot share parameters in HAPPO, which significantly affects the training efficiency in complex tasks.

Table 2: Mean value and standard deviation of winning rate on the SMAC benchmark.

Task	Difficulty	T-PPO	T-PPO-D	MAPPO	HAPPO	QPLEX
MMM2	Super Hard	81.6 (7.7)	82.5 (6.1)	68.5 (8.4)	56.1 (39.6)	74.8 (11.6)
3s5z vs 3s6z	Super Hard	85.5 (5.2)	82.7 (6.2)	78.3 (14.5)	21.8 (11.1)	75.8 (12.3)
6h vs 8z	Super Hard	91.8 (1.1)	78.6 (4.1)	90.7 (0.7)	0.5 (0.1)	20.7 (14.7)
corridor	Super Hard	99.1 (0.3)	99.2 (0.1)	97.9 (0.4)	7.8 (11.0)	30.3 (41.3)
3h vs 1b1z3h	Local Optimal	71.4 (20.7)	65.9 (17.2)	35.0 (31.6)	1.9 (1.4)	30.7 (23.2)
1c3s5z	Easy	99.8 (0.0)	99.8 (0.1)	73.3 (11.4)	99.9 (0.0)	98.7 (1.0)

We show the mean and standard deviation between the winning rates of the final policies trained on different random seeds in Table 2. T-PPO-Distillation (T-PPO-D) outperforms T-PPO in two maps while outperforming MAPPO in five out of six maps, indicating our approach’s competitiveness in decentralized execution. Only in 6h_vs_8z, T-PPO-Distillation performs worse than T-PPO, demonstrating that correlation learned by T-PPO might be overly dependent on the sequential transformation even though we have added several normalization items. Although this phenomenon rarely occurs and depends on one special task, we will study this limitation in future work.

5.2.1 Advantage of Sequential Transformation Framework in SMAC

In this section, we will further analyze the local optimality of SMAC. Compared with the matrix game, the StarCraft II tasks are more complex with high dimensional state space. To verify whether our approach can drive agents out of local optimal points as in matrix games, we create a new StarCraft II map named 3h_vs_1b1z3h.

In 3h_vs_1b1z3h, we control three Hydralisks, while our opponent controls three Hydralisks, one low damage Zergling, and one Baneling with high area damage. The explosion of the Baneling can only be avoided if all agents gather fire to it instead of the nearer Zergling. However, gathering fire to the Zergling could be a suboptimal equilibrium, where no-agent is tending to change its policy.

Previous research has demonstrated super hard maps in SMAC require more exploration [Wang et al., 2020, Li et al., 2021a]. However, we find different experimental results on the maps that contain local optimal points, such as our own designed map 3h_vs_1b1z3h. In PPO, explo-



Figure 4: Illustration of 3h_vs_1b1z3h.

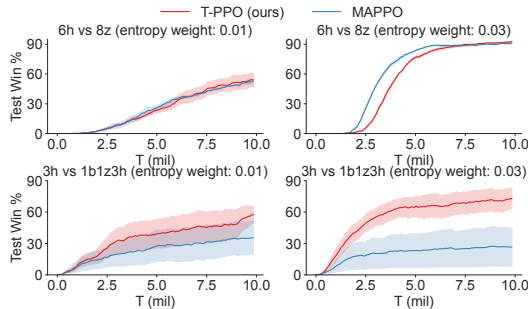


Figure 5: Different changes caused by adjusting the exploration coefficients (entropy weight) between T-PPO and MAPPO on 3h_vs_1b1z3h and 6h_vs_8z.

ration is guaranteed by the entropy term in its loss function. As shown in Figure 5, T-PPO and MAPPO’s performance changes are divergent on different maps while tuning the related hyperparameter. On 6h_vs_8z, increasing entropy weight will bring improvement in learning efficiency for both algorithms. It is in line with our expectations. On 3h_vs_1b1z3h, increasing entropy weight will still improve the performance of T-PPO, but will make the performance of MAPPO worse. We believe this phenomenon is related to the local optimality we discussed above. MAPPO has no motion to drive agents to escape local optimal points, which leads to low exploitation efficiency. Taking the advantage of handling global optimality as discussed in Section 4.1, our approach achieves better exploitation under the same exploration strategy.

5.3 Google Research Football

In this section, we further test our approach against policy-based baselines on another MARL benchmark named Google Research Football (GRF). In the environment setting, we use sparse rewards with both SCORING and CHECKPOINT for our approach and all baselines. For observations, we follow [Li et al., 2021a], using simple 115 as the observation while removing the information irrelevant to the current scenario. Meanwhile, we introduce the relative position for each agent instead of absolute coordinates to achieve a more realistic environment.

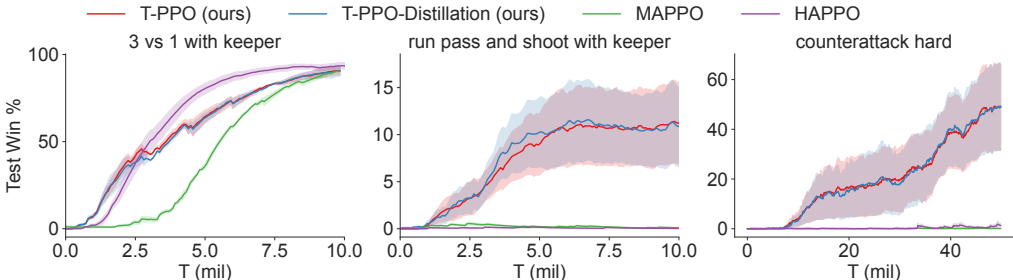


Figure 6: Learning curve of GRF.

As shown in Figure 6, our approach obviously outperforms baselines, achieving remarkable winning rate while baselines almost learn nothing to win in academy_pass_and_shoot_with_keeper and academy_counterattack_hard. In GRF scenarios, agents need to coordinate timing and positions for organizing offense to seize fleeting opportunities. The cooperation between agents is difficult to coordinate because of the sparsity of agents’ crucial movements. Our sequential transformation framework provides an optimal solution on MMDP by forcing agents to consider the information from previous ones, which promotes coordination among agents for achieving sophisticated cooperation. Compared with T-PPO, T-PPO-Distillation performs similarly, which ensures that our algorithm can be executed in a wide range of environments.

6 Conclusion

In this paper, we study state-of-the-art cooperative multi-agent reinforcement learning methods and observe that, even with the full expressiveness, they may fail to converge to an optimal solution in simple matrix games. To analyze this phenomenon, we generalize these MARL methods with a general model and find that their factorized policy structure combined with the gradient descent optimization is one of the major causes of their suboptimality. To solve this issue, we propose a novel sequential transformation framework that allows employing off-the-shelf single-agent reinforcement learning methods to solve cooperative multi-agent tasks and retain their global optimality guarantee. Based on this framework, we develop T-PPO that extends single-agent PPO to multi-agent settings and significantly outperforms baselines on a variety of benchmark tasks. It is an interesting future direction to extend efficient value-based SARL methods to multi-agent settings through our transformation framework.

References

- J. Alonso-Mora, S. Baker, and D. Rus. Multi-robot formation control and object transport in dynamic environments via constrained optimization. *The International Journal of Robotics Research*, 36(9): 1000–1021, 2017.
- C. Boutilier. Planning, learning and coordination in multiagent decision processes. In *Proceedings of the 6th Conference on Theoretical Aspects of Rationality and Knowledge*, pages 195–210. Morgan Kaufmann Publishers Inc., 1996.
- C. S. de Witt, T. Gupta, D. Makoviichuk, V. Makoviychuk, P. H. Torr, M. Sun, and S. Whiteson. Is independent learning all you need in the starcraft multi-agent challenge? *arXiv preprint arXiv:2011.09533*, 2020.
- J. N. Foerster, G. Farquhar, T. Afouras, N. Nardelli, and S. Whiteson. Counterfactual multi-agent policy gradients. In *AAAI*, 2018.
- L. Kraemer and B. Banerjee. Multi-agent reinforcement learning as a rehearsal for decentralized planning. *Neurocomputing*, 190:82–94, 2016a.
- L. Kraemer and B. Banerjee. Multi-agent reinforcement learning as a rehearsal for decentralized planning. *Neurocomputing*, 190:82–94, 2016b.
- J. G. Kuba, R. Chen, M. Wen, Y. Wen, F. Sun, J. Wang, and Y. Yang. Trust region policy optimisation in multi-agent reinforcement learning. *arXiv preprint arXiv:2109.11251*, 2021.
- K. Kurach, A. Raichuk, P. Stańczyk, M. Zajac, O. Bachem, L. Espeholt, C. Riquelme, D. Vincent, M. Michalski, O. Bousquet, et al. Google research football: A novel reinforcement learning environment. *arXiv preprint arXiv:1907.11180*, 2019.
- C. Li, C. WU, T. Wang, J. Yang, Q. Zhao, and C. Zhang. Celebrating diversity in shared multi-agent reinforcement learning. *arXiv preprint arXiv:2106.02195*, 2021a.
- G. Li, C. Cai, Y. Chen, Y. Gu, Y. Wei, and Y. Chi. Is q-learning minimax optimal? a tight sample complexity analysis, 2021b.
- B. Liu, Q. Cai, Z. Yang, and Z. Wang. Neural proximal/trust region policy optimization attains globally optimal policy, 2019. URL <https://arxiv.org/abs/1906.10306>.
- R. Lowe, Y. Wu, A. Tamar, J. Harb, P. Abbeel, and I. Mordatch. Multi-agent actor-critic for mixed cooperative-competitive environments. *Neural Information Processing Systems (NIPS)*, 2017.
- X. Ma, Y. Yang, C. Li, Y. Lu, Q. Zhao, and Y. Jun. Modeling the interaction between agents in cooperative multi-agent reinforcement learning. *arXiv preprint arXiv:2102.06042*, 2021.
- V. Mnih, K. Kavukcuoglu, D. Silver, A. Graves, I. Antonoglou, D. Wierstra, and M. Riedmiller. Playing atari with deep reinforcement learning, 2013. URL <https://arxiv.org/abs/1312.5602>.
- F. A. Oliehoek, M. T. Spaan, and N. Vlassis. Optimal and approximate q-value functions for decentralized pomdps. *Journal of Artificial Intelligence Research*, 32:289–353, 2008.
- F. A. Oliehoek, C. Amato, et al. *A concise introduction to decentralized POMDPs*, volume 1. Springer, 2016.
- T. Rashid, M. Samvelyan, C. S. D. Witt, G. Farquhar, J. N. Foerster, and S. Whiteson. Qmix: Monotonic value function factorisation for deep multi-agent reinforcement learning. *ArXiv*, abs/1803.11485, 2018.
- M. Samvelyan, T. Rashid, C. S. D. Witt, G. Farquhar, N. Nardelli, T. G. J. Rudner, C.-M. Hung, P. H. S. Torr, J. N. Foerster, and S. Whiteson. The starcraft multi-agent challenge. *ArXiv*, abs/1902.04043, 2019.
- J. Schulman, F. Wolski, P. Dhariwal, A. Radford, and O. Klimov. Proximal policy optimization algorithms. *ArXiv*, abs/1707.06347, 2017a.

- J. Schulman, F. Wolski, P. Dhariwal, A. Radford, and O. Klimov. Proximal policy optimization algorithms. *arXiv preprint arXiv:1707.06347*, 2017b.
- K. Son, D. Kim, W. J. Kang, D. E. Hostallero, and Y. Yi. Qtran: Learning to factorize with transformation for cooperative multi-agent reinforcement learning. *ArXiv*, abs/1905.05408, 2019.
- P. Sunehag, G. Lever, A. Gruslys, W. M. Czarnecki, V. F. Zambaldi, M. Jaderberg, M. Lanctot, N. Sonnerat, J. Z. Leibo, K. Tuyls, and T. Graepel. Value-decomposition networks for cooperative multi-agent learning. *ArXiv*, abs/1706.05296, 2018.
- R. S. Sutton and A. G. Barto. *Reinforcement learning: An introduction*. MIT press, 2018.
- E. Van der Pol and F. A. Oliehoek. Coordinated deep reinforcement learners for traffic light control. *Proceedings of Learning, Inference and Control of Multi-Agent Systems (at NIPS 2016)*, 2016.
- J. Wang, Z. Ren, B. Han, J. Ye, and C. Zhang. Towards understanding cooperative multi-agent q-learning with value factorization. *Advances in Neural Information Processing Systems*, 34, 2021a.
- J. Wang, Z. Ren, T. Liu, Y. Yu, and C. Zhang. Qplex: Duplex dueling multi-agent q-learning. *ArXiv*, abs/2008.01062, 2021b.
- T. Wang, T. Gupta, A. Mahajan, B. Peng, S. Whiteson, and C. Zhang. Rode: Learning roles to decompose multi-agent tasks. *arXiv preprint arXiv:2010.01523*, 2020.
- Y. Wang, B. Han, T. Wang, H. Dong, and C. Zhang. Dop: Off-policy multi-agent decomposed policy gradients. In *ICLR*, 2021c.
- C. Yu, A. Velu, E. Vinitsky, Y. Wang, A. Bayen, and Y. Wu. The surprising effectiveness of ppo in cooperative, multi-agent games. *arXiv preprint arXiv:2103.01955*, 2021.
- C. Zhang and V. Lesser. Coordinated multi-agent reinforcement learning in networked distributed pomdps. In *Twenty-Fifth AAAI Conference on Artificial Intelligence*, 2011.

A Appendix

A.1 Instances of GPF-MAC

We will show that most existing MARL algorithms are instances of GPF-MAC. For actor-critic algorithms, it's quite straightforward. For value-based algorithms, their individual action value networks Q_i can be viewed as the "actor" in GPF-MAC: θ_i is the parameters of Q_i , the policy is derived by $\pi(s) = \arg \max Q_i(s, \cdot; \theta_i)$. The function C in actor-critic method is just the expected return of current policy, as for value-decomposition methods, it is usually the TD-loss function.

COMA, MADDPG, MAPPO, DOP These algorithms are all actor-critic algorithms. Similarly for these algorithms, θ_i is the network parameters of i -th individual local policy networks. $C(\theta_1, \dots, \theta_n) = -\mathcal{J}(\pi_{\theta_1}, \dots, \pi_{\theta_n})$ is the opposite number of the expected return of current joint policy. What differs MADDPG from the other three algorithms is that MADDPG uses the parameterized deterministic policy as its policy, while the others uses stochastic policies. The difference between COMA, MAPPO and DOP is that they uses different \mathcal{E} as their optimization method. First, they all try to learn a critic to approximate the value of current policy, and further, to approximate the policy gradient. What different is, for COMA, Lemma 1 in [Foerster et al., 2018] shows that \mathcal{E} in COMA is some variant of stochastic gradient descent (i.e. the expectation of the update vector is true policy gradient providing the critic is accurate), they use a counterfactual baseline to derive a new estimation method for the gradient; for MAPPO, a regularizer to the policy gradient is used to tackle monotonic improvement of the policy value; for DOP, a monotonic critic is used to approximate the true value function, and the estimation of policy gradient is thus biased.

VDN, QMIX, QPLEX For these algorithms, θ_i is the parameter of individual action-value network Q_i . We remind of that in actor-critic methods, we deal with the critic by viewing it as the approximation of the true value of current policy, the learning process of such approximation is put into \mathcal{E} as a part of the optimization method. In QMIX and QPLEX, there are also extra parameters other than their "actor"s – the individual action-value networks, that is, their parameter in mixing networks. We can deal with them as an auxiliary agent which doesn't affect the dynamics of the environment and the return of the policy while only affects the calculation of C . For example, let ϕ be the parameters in mixing network of VDN, QMIX or QPLEX (in VDN, $\phi = \emptyset$, we don't need an auxiliary agent), then we have $C(\theta_1, \dots, \theta_n, \phi) = \mathbb{E}_{s, \mathbf{a}, r, s'} [\text{mixer}(Q_i(s, a_i); \phi) - r - \gamma \text{mixer}(\max Q_i(s', \cdot); \phi)]^2$ – the TD-loss function. One can also deal parameters in the critic of actor-critic algorithms like this, however, we think it's more natural to view this approximation as a part of optimization method \mathcal{E} .

QTRAN QTRAN is actually very similar to actor-critic algorithms. We follow the notations in [Son et al., 2019], then Q_{jt} is actually a critic approximating the value of current policy. θ_i is the parameter of individual action-value network Q_i , $C(\theta_1, \dots, \theta_n) = L_{\text{opt}} + L_{\text{nopt}}$ evaluates how good current policy is w.r.t. the critic Q_{jt} (the minimum of C is attained only if Q_i s constitute the greedy policy w.r.t. Q_{jt}).

A.2 Suboptimality of Existing GPF-MAC

For actor-critic instances of GPF-MAC, we recall proposition 3.1:

Proposition 3.1. *For the actor-critic instance of GPF-MAC optimized by gradient descent, any Nash's Equilibrium of policies is a stationary point.*

Proof. Suppose $(\pi_{\theta_1}, \dots, \pi_{\theta_n})$ is an NE, then by the definition of NE, we have $\forall i = 1, \dots, n : \forall \theta'_i : \mathcal{J}(\pi_{\theta_1}, \dots, \pi_{\theta_n}) \geq \mathcal{J}(\pi_{\theta_1}, \dots, \pi_{\theta_{i-1}}, \pi_{\theta'_i}, \pi_{\theta_{i+1}}, \dots, \pi_{\theta_{-i}})$.

By definition of C of actor-critic instances of GPF-MAC, it's equivalent to $\forall i = 1, \dots, n : \forall \theta'_i : C(\theta_1, \dots, \theta_n) \leq C(\theta_1, \dots, \theta_{i-1}, \theta'_i, \theta_{i+1}, \dots, \theta_{-i})$.

Suppose $\exists i : \frac{\partial C}{\partial \theta_i} \neq \mathbf{0}$. Let $l = (\underbrace{\mathbf{0}, \dots, \mathbf{0}}_{i-1}, \frac{\partial C}{\partial \theta_i}, \underbrace{\mathbf{0}, \dots, \mathbf{0}}_{n-i})$, we have

$$\lim_{\delta \rightarrow 0} \frac{C((\theta_1, \dots, \theta_n) + \delta l) - C(\theta_1, \dots, \theta_n)}{\delta \|l\|_2} = \|l\|_2 \neq 0$$

Choose a sufficient small δ will constitute a contradiction of the definition of NE. Thus we have $\forall i : \frac{\partial C}{\partial \theta_i} = \mathbf{0}$.

After that, by applying the derivation rule of compound function,

$$\frac{\partial C}{\partial \Theta} = \sum_{i=1}^n \frac{\partial C}{\partial \theta_i} \frac{\partial \theta_i}{\partial \Theta} = \mathbf{0}$$

we can address the situation where parameter-sharing is taken into consideration, which completes our proof. \square

For each specific algorithm, there are two gaps for them to realize optimality:

1. Is \mathcal{E} able to calculate the global optimum of C ?
2. Does the global optimum of C constitutes the global optimal policy?

COMA, MADDPG, MAPPO, DOP For actor-critic algorithms, the second gap is naturally filled since $C = -\mathcal{J}$. For COMA, MAPPO and MADDPG, their critic can be any approximator, if we assume this approximator converges eventually, then the first gap can be produced by NEs of policies (proposition 3.1). For DOP, its critic is a monotonic network, so it fails when the best policy of the monotonic approximation is not equal to the true best policy.

VDN, QMIX For VDN and QMIX, the second gap is created when the value function is not additive or monotonic.

QPLEX The second gap of QPLEX is filled due to its completeness of function class. However, its complex structure creates numerous local minimums of C , which creates the gap of the first kind when variants of gradient descent methods are used. Actually, we have the following proposition

Proposition A.1. *In QPLEX, for any MMDP with no cycle, for arbitrary non-degenerated $\theta_1, \dots, \theta_n$, we can find a ϕ such that $(\theta_1, \dots, \theta_n, \phi)$ constitutes a local optimum of C , where ϕ is the parameter of the auxiliary agent mentioned in appendix A.1. The term "non-degenerated" of θ_i refers to the uniqueness of the greedy action w.r.t. $Q_i(s, \cdot)$.*

Proof. For simplicity, we simplify the formula of QPLEX as follows. A full proof has no technical difference in essence.

The mixing network of QPLEX can be simplified as

$$Q(s, \mathbf{a}; \theta_1, \dots, \theta_n, \phi) = b(s; \phi) + \lambda(s, \mathbf{a}; \phi) \sum A_i(s, a_i; \phi)$$

where $A_i(s, a_i; \phi) = Q_i(s, a_i; \phi) - \max Q_i(s, \cdot; \phi)$, $\lambda(s, \mathbf{a}; \phi) \geq 0$.

Denote $T(s, \mathbf{a}) = r(s, \mathbf{a}) + \gamma \mathbb{E}_{s' \sim P(s, \mathbf{a})} [\max Q(s, \cdot)]$ as the target.

Now we want to find a local minimum of C . Since a sufficient small neighborhood of $(\theta_1, \dots, \theta_n, \phi)$ where $\theta_1, \dots, \theta_n$ are non-degenerated won't change the policy, we can fix $\mathbf{a}^*(s) = \arg \max Q(s, \cdot)$ for each state s ($\mathbf{a}^*(s)$ is abbreviated as \mathbf{a}^* when there is no ambiguity).

Then for any state s , for each $\mathbf{a} \neq \mathbf{a}^*$ satisfying $T(s, \mathbf{a}) \leq T(s, \mathbf{a}^*)$, the best we can expect is $Q(s, \mathbf{a}) = T(s, \mathbf{a})$; for each \mathbf{a} satisfying $T(s, \mathbf{a}) > T(s, \mathbf{a}^*)$, the best we can expect is $Q(s, \mathbf{a}) = V(s)$.

λ only affects the advantage, so its sufficient to set

$$\lambda(s, \mathbf{a}; \phi) = \min(T(s, \mathbf{a}) - T(s, \mathbf{a}^*), 0) / \sum_i A_i(s, a_i; \phi)$$

b only affects the value, so we need to ensure

$$b(s; \phi) = \frac{1}{K(s) + 1} \sum_{\mathbf{a}} \max(T(s, \mathbf{a}) - T(s, \mathbf{a}^*), 0) + T(s, \mathbf{a}^*)$$

to minimize the sum of squared distance, where $K(s) = \#\{T(s, \mathbf{a}) > T(s, \mathbf{a}^*)\}$.

It worth noting that a modification of b might change T , the equations of b might be unsatisfiable. However, for acyclic MMDPs, we can calculate b by the reversal of topological order, which completes our proof.

□

In empirical design of the algorithm, we notice that QPLEX has used some engineering tricks like "stop gradient" to modify the gradient of non-optimal points helping the algorithm to jump out of some local optimums. But these tricks are lack of theoretical guarantee, we can still construct cases that QPLEX is not able to reach global optimum, such as the following Matrix Game (Table3).

-20	10
10	9

Table 3: Matrix Game 2, $m = 2$

This Matrix Game has two global optimums (0, 1) and (1, 0), and a suboptimal solution (1, 1) with high reward. QPLEX will likely to initialize to the suboptimal solution (1, 1), and after that, it get confused since the manually modified gradient doesn't tell it the right direction. The learnt joint Q vibrates around the following matrix:

$$\begin{pmatrix} -20 & 29/3 - \epsilon \\ 29/3 - \epsilon & 29/3 \end{pmatrix}$$

which can be proved to be a local optimum of C according to the proof of proposition A.1.

QTRAN C in QTRAN is discontinuous, for everywhere the police switches may constitute a jump discontinuity, which may be harmful for gradient descent methods, since gradient descent methods assume the loss function to be differentiable. Unfortunately, we are not able to give any theoretical analysis about QTRAN, either prove or disprove its optimality. We have only empirical results shown in section 5 to prove its potential suboptimality.

A.3 Sequential Transformation

A.3.1 Pseudocode of the framework with sequential transformation

Here we present pseudo-code of the sequential framework (Algorithm algorithm 2).

A.3.2 Proof of theorem 4.1

Here we present the proof of theorem 4.1.

Theorem 4.1. *For any deterministic policy π on $\Gamma(\mathcal{M})$, there is a decentralized policy $\pi_{jt} = (\pi_1, \dots, \pi_N)$ on \mathcal{M} such that $\mathcal{J}_{\mathcal{M}}(\pi_{jt}) = \gamma^{(1-n)/n} \mathcal{J}_{\Gamma(\mathcal{M})}(\pi)$, where $\pi_1(s) = \pi(s)$, $\pi_k(s) = \pi((s, \pi_1(s), \dots, \pi_{k-1}(s)))$ for all $k > 1$.*

For any stochastic policy η on $\Gamma(\mathcal{M})$, there is a communicated policy $\eta_{jt} = (\eta_1, \dots, \eta_N)$ on \mathcal{M} such that $\mathcal{J}_{\mathcal{M}}(\eta_{jt}) = \gamma^{(1-n)/n} \mathcal{J}_{\Gamma(\mathcal{M})}(\eta)$, where $\eta_1(a_1|s) = \eta(a_1|s)$, $\eta_k(a_k|s, a_1, \dots, a_{k-1}) = \eta(a_k|(s, a_1, \dots, a_{k-1}))$ for all $k > 1$, where a_1, \dots, a_{k-1} are actions selected by agents $1, \dots, k-1$.

And conversely, for any policy π_{jt} on \mathcal{M} , there is a policy π on $\Gamma\mathcal{M}$ such that $\mathcal{J}_{\mathcal{M}}(\pi_{jt}) = \gamma^{(1-n)/n} \mathcal{J}_{\Gamma(\mathcal{M})}(\pi)$.

Algorithm 2 The Sequential Framework

```

1: Input: An SARL algorithm  $\mathfrak{A}$ , an oracle  $O^{\mathcal{M}}$  for interaction with an MMDP  $\mathcal{M}$ .
2: while Simulating  $\mathfrak{A}$  do
3:   if  $\mathfrak{A}$  asks for the initialization of environment then
4:     Initialize  $t = 0$ ,  $a_i = 0$  for  $i = 1, \dots, N$ .
5:     Call  $O^{\mathcal{M}}$  for the initialization of  $\mathcal{M}$  and obtain  $s_0$ 
6:     Return  $s_0$  to  $\mathfrak{A}$ .
7:   else if  $\mathfrak{A}$  asks for an interaction with the environment by providing an action  $a$  then
8:      $a_{t \bmod N+1} \leftarrow a$ 
9:     if  $t \bmod N = N - 1$  then
10:      Call  $O^{\mathcal{M}}$  for the interaction by providing action  $(a_1, \dots, a_N)$  to obtain reward  $r$  and
      next state  $s'$ .
11:       $s \leftarrow s'$ 
12:      Return  $r$  and  $s'$  to  $\mathfrak{A}$ .
13:   else
14:     Return 0 and  $(s, a_1, \dots, a_{t \bmod N+1})$  to  $\mathfrak{A}$ .
15:   end if
16:    $t = t + 1$ 
17:   else if  $\mathfrak{A}$  returns an policy  $\pi$  then
18:     Convert  $\pi$  to the joint policy  $\pi_{\text{jt}}$  on  $\mathcal{M}$ .
19:     Break
20:   end if
21: end while
22: Return  $\pi_{\text{jt}}$ .

```

Proof. For deterministic policy:

$$\begin{aligned}
\mathcal{J}_{\mathcal{M}}(\pi_{\text{jt}}) &= \mathbb{E} \left[\sum_{t=0}^{\infty} \gamma^t r(s_t, \pi_{\text{jt}}) \middle| s_{t+1} \sim P(s_t, \pi_{\text{jt}}) \right] \\
&= \mathbb{E} \left[\sum_{t=0}^{\infty} \tilde{\gamma}^{nt} \tilde{r}((s_t, \pi_1(s_t), \dots, \pi_{n-1}(s_t)), \pi) \middle| s_{t+1} \sim P(s_t, \pi_{\text{jt}}) \right] \\
&= \mathbb{E} \left[\sum_{t=0}^{\infty} \sum_{k=0}^{n-1} \tilde{\gamma}^{nt+k-n+1} \tilde{r}((s_t, \pi_1(s_t), \dots, \pi_{k-1}(s_t)), \pi) \middle| s_{t+1} \sim P(s_t, \pi_{\text{jt}}) \right] \\
&= \mathbb{E} \left[\tilde{\gamma}^{1-n} \sum_{t'=0}^{\infty} \tilde{\gamma}^{t'} \tilde{r}(s_{t'}, \pi) \middle| s_{t'+1} \sim \tilde{P}(s_{t'}, \pi) \right] \\
&= \gamma^{\frac{1-n}{n}} J_{\Gamma(\mathcal{M})}(\pi)
\end{aligned}$$

For stochastic policy the proof is similar,

$$\begin{aligned}
\mathcal{J}_{\mathcal{M}}(\eta_{jt}) &= \mathbb{E} \left[\sum_{t=0}^{\infty} \gamma^t r(s_t, \eta_{jt}) \middle| s_{t+1} \sim P(s_t, \eta_{jt}) \right] \\
&= \mathbb{E} \left[\sum_{t=0}^{\infty} \tilde{\gamma}^{nt} \tilde{r} \left(\left(s_t, a_{<n}^{(t)} \right), \eta \right) \middle| s_{t+1} \sim P(s_t, \eta_{jt}), a_l^{(t)} \sim \eta \left(\cdot \middle| \left(s_t, a_{<l}^{(t)} \right) \right) \right] \\
&= \mathbb{E} \left[\sum_{t=0}^{\infty} \sum_{k=0}^{n-1} \tilde{\gamma}^{nt+k-n+1} \tilde{r} \left(\left(s_t, a_{<k}^{(t)} \right), \eta \right) \middle| s_{t+1} \sim P(s_t, \eta_{jt}), a_l^{(t)} \sim \eta \left(\cdot \middle| \left(s_t, a_{<l}^{(t)} \right) \right) \right] \\
&= \mathbb{E} \left[\tilde{\gamma}^{1-n} \sum_{t'=0}^{\infty} \tilde{\gamma}^{t'} \tilde{r}(s_{t'}, \eta) \middle| s_{t'+1} \sim \tilde{P}(s_{t'}, \eta) \right] \\
&= \gamma^{\frac{1-n}{n}} J_{\Gamma(\mathcal{M})}(\eta)
\end{aligned}$$

For the converse part of the theorem, suppose $\pi_{jt} = (\pi_1, \dots, \pi_n)$, it's sufficient to let $\pi((s, a_1, \dots, a_{k-1})) = \pi_k(s)$. The calculation of its value is similar to the above, we omit it here. □

A.4 An Extension of Q-learning

Here we introduce a variant of Q-learning dealing with deterministic transitions (algorithm 3) to demonstrate the claim at the end of section 4.2. If we adopt this algorithm in our sequential transformation framework, it will have the same sample complexity as the original Q-learning on the original MMDP \mathcal{M} .

We denote $D : \mathcal{S} \times \mathcal{A} \rightarrow \{0, 1\}$ as an oracle telling whether this state-action pair would result in a deterministic transition.

Algorithm 3 QLDT (Q-learning for MDPs with deterministic transitions)

Access to: An oracle $D : \mathcal{S} \times \mathcal{A} \rightarrow \{0, 1\}$.
Initialize Q
for $t \leftarrow 0$ **to** T **do**
 $s \leftarrow s_0$
 Initialize stack v .
 for each step of epoch t **do**
 $a \leftarrow \text{SelectAction}(\pi, s)$ $\{\epsilon\text{-greedy}\}$
 $r \leftarrow \text{Reward}(s, a)$
 $s' \leftarrow \text{NextState}(s, a)$
 if $D(s, a)$ **then**
 Push (s, a, r, s') into v $\{\text{deterministic transition}\}$
 $Q(\tilde{s}, \tilde{a}) \leftarrow \tilde{r} + \gamma \max Q(\tilde{s}', \cdot)$
 else
 $Q(s, a) \leftarrow Q(s, a) + \alpha[r + \gamma \max Q(s', \cdot) - Q(s, a)]$
 while v is not empty **do**
 Pop v to get $(\tilde{s}, \tilde{a}, \tilde{r}, \tilde{s}')$
 $Q(\tilde{s}, \tilde{a}) \leftarrow \tilde{r} + \gamma \max Q(\tilde{s}', \cdot)$
 end while
 end if
 $s \leftarrow s'$
 end for
end for

We have proposition A.2.

Proposition A.2. *T-QLDT has the same sample complexity as original Q-learning on \mathcal{M} .*

Proof. One can view T-QLDT as the original Q-learning maintaining a max heap, where $Q((s, a_1, \dots, a_{k-1}), a_k) = \max Q((s, a_1, \dots, a_k), \cdot)$. In this way, T-QLDT has exactly the same behaviour as the original Q-learning and does not change the sample complexity as a consequence. \square

A.5 The minimax sample complexity of the sequential framework

Here we explain a bit more of the claim of the minimax sample complexity in section 4.2.

The minimax sample complexity here is the sample complexity of the "best" algorithm over the "hardest" task. For any multi-agent algorithm A , we can always find a single-agent algorithm B , such that $A = T-B$. It is because that for any MDP $\tilde{\mathcal{M}}$, we can always compress n steps on $\tilde{\mathcal{M}}$ into one step, and then use the corresponding multi-agent algorithm A to solve it as a multi-agent problem. In this way, $T-B$ is exactly A , and thus not increase the minimax sample complexity. One should keep in mind that every n samples on MDP correspond to exactly one sample on MMDP. Particularly, the number of bits we need to record every n samples on MDP are exactly what we need to record one sample on MMDP.

B Experimental Details

In this section, we provide more experimental results supplementary to those presented in Section 5. We also discuss the details of the experimental settings of both our matrix game and the StarCraft II micromanagement (SMAC) benchmark.

B.1 Multi-task Matrix Game

In section 5.1, we design a multi-task matrix game to demonstrate the global optimality of our sequential transformation framework. In this section, we will first show the details of this environment and provide more evidence of our algorithms' advantage on MMDP.

B.1.1 Details of Multi-task Matrix Game

In multi-task matrix game, the return of the optimal strategy corresponding to each matrix is 10, which means the sum rewards of the global optimal strategy is 100. Two agents are initialized to one matrix uniformly at random, and the ID of a current matrix is observable to both of them. They need to cooperate to select the entry with the maximum reward for the current matrix, after that, the game ends. Each matrix contains $5 \times 5 = 25$ entries, which means $\mathcal{A} = \{0, 1, 2, 3, 4\}$ for each agent.

All 10 payoff matrices are listed in table 4. The optimal strategies' payoff of all matrices is 10. Matrices 1 – 5 are hand-crafted in order to create some hard NEs. Matrices 6 – 10 are drawn uniformly at random. It's worth noting that a random 5×5 matrix has $25/9 \approx 2.77$ different NEs in expectation. And in our opinion, the existence of suboptimal NEs is the main reason why existing algorithms fail.

B.1.2 Visualization of Learned Joint Strategies

Table 5: Payoff matrix				Table 6: π_{tot} of TPPO				Table 7: π_{tot} of MAPPO			
$a_2 \backslash a_1$	$\mathcal{A}^{(1)}$	$\mathcal{A}^{(2)}$	$\mathcal{A}^{(3)}$	$a_2 \backslash a_1$	$\mathcal{A}^{(1)}$	$\mathcal{A}^{(2)}$	$\mathcal{A}^{(3)}$	$a_2 \backslash a_1$	$\mathcal{A}^{(1)}$	$\mathcal{A}^{(2)}$	$\mathcal{A}^{(3)}$
$\mathcal{A}^{(1)}$	8	-12	-12	$\mathcal{A}^{(1)}$	1	0	0	$\mathcal{A}^{(1)}$	0	0	0
$\mathcal{A}^{(2)}$	-12	0	0	$\mathcal{A}^{(2)}$	0	0	0	$\mathcal{A}^{(2)}$	0	0.2	0.2
$\mathcal{A}^{(3)}$	-12	0	0	$\mathcal{A}^{(3)}$	0	0	0	$\mathcal{A}^{(3)}$	0	0.3	0.3

To further illustrate our approach's ability to attach the global optimal point, we use the matrix game in [Wang et al., 2021b, Ma et al., 2021] as a toy example (shown in Table 5). Here we compare our approach T-PPO with MAPPO. Joint policies learned by T-PPO and MAPPO are shown in Table 6 and Table 7. MAPPO falls into local optimal points due to proposition 3.1, while T-PPO obtains the optimal strategy. Taking this advantage, our approach dominates in our multi-task matrix game.

Table 4: Multi-task Matrix Game

Matrix 1						Matrix 2					
$a_2 \backslash a_1$	$\mathcal{A}^{(1)}$	$\mathcal{A}^{(2)}$	$\mathcal{A}^{(3)}$	$\mathcal{A}^{(4)}$	$\mathcal{A}^{(5)}$	$a_2 \backslash a_1$	$\mathcal{A}^{(1)}$	$\mathcal{A}^{(2)}$	$\mathcal{A}^{(3)}$	$\mathcal{A}^{(4)}$	$\mathcal{A}^{(5)}$
$\mathcal{A}^{(1)}$	10	-10	-10	-10	-10	$\mathcal{A}^{(1)}$	10	-10	10	-10	10
$\mathcal{A}^{(2)}$	-10	9	0	0	0	$\mathcal{A}^{(2)}$	-10	10	-10	10	-10
$\mathcal{A}^{(3)}$	-10	0	9	0	0	$\mathcal{A}^{(3)}$	10	-10	10	-10	10
$\mathcal{A}^{(4)}$	-10	0	0	9	0	$\mathcal{A}^{(4)}$	-10	10	-10	10	-10
$\mathcal{A}^{(5)}$	-10	0	0	0	9	$\mathcal{A}^{(5)}$	10	-10	10	-10	10

Matrix 3						Matrix 4					
$a_2 \backslash a_1$	$\mathcal{A}^{(1)}$	$\mathcal{A}^{(2)}$	$\mathcal{A}^{(3)}$	$\mathcal{A}^{(4)}$	$\mathcal{A}^{(5)}$	$a_2 \backslash a_1$	$\mathcal{A}^{(1)}$	$\mathcal{A}^{(2)}$	$\mathcal{A}^{(3)}$	$\mathcal{A}^{(4)}$	$\mathcal{A}^{(5)}$
$\mathcal{A}^{(1)}$	-20	-20	-20	-20	10	$\mathcal{A}^{(1)}$	-20	-20	-20	-20	10
$\mathcal{A}^{(2)}$	-20	-20	-20	10	9	$\mathcal{A}^{(2)}$	-20	-20	-20	10	9
$\mathcal{A}^{(3)}$	-20	-20	10	9	9	$\mathcal{A}^{(3)}$	-20	-20	10	9	8
$\mathcal{A}^{(4)}$	-20	10	9	9	9	$\mathcal{A}^{(4)}$	-20	10	9	8	7
$\mathcal{A}^{(5)}$	10	9	9	9	9	$\mathcal{A}^{(5)}$	10	9	8	7	6

Matrix 5						Matrix 6					
$a_2 \backslash a_1$	$\mathcal{A}^{(1)}$	$\mathcal{A}^{(2)}$	$\mathcal{A}^{(3)}$	$\mathcal{A}^{(4)}$	$\mathcal{A}^{(5)}$	$a_2 \backslash a_1$	$\mathcal{A}^{(1)}$	$\mathcal{A}^{(2)}$	$\mathcal{A}^{(3)}$	$\mathcal{A}^{(4)}$	$\mathcal{A}^{(5)}$
$\mathcal{A}^{(1)}$	-20	-15	-10	-5	6	$\mathcal{A}^{(1)}$	0.8	-16.0	-5.0	-10.9	-3.7
$\mathcal{A}^{(2)}$	-20	-15	-10	7	5	$\mathcal{A}^{(2)}$	-9.2	-4.2	7.3	9.6	-3.0
$\mathcal{A}^{(3)}$	-20	-15	8	6	4	$\mathcal{A}^{(3)}$	-20.0	-18.1	0.2	-4.3	9.0
$\mathcal{A}^{(4)}$	-20	9	7	5	3	$\mathcal{A}^{(4)}$	-14.9	-2.0	-17.7	-17.6	-0.8
$\mathcal{A}^{(5)}$	10	8	6	4	2	$\mathcal{A}^{(5)}$	3.8	10	7.5	9.2	-10.7

Matrix 7						Matrix 8					
$a_2 \backslash a_1$	$\mathcal{A}^{(1)}$	$\mathcal{A}^{(2)}$	$\mathcal{A}^{(3)}$	$\mathcal{A}^{(4)}$	$\mathcal{A}^{(5)}$	$a_2 \backslash a_1$	$\mathcal{A}^{(1)}$	$\mathcal{A}^{(2)}$	$\mathcal{A}^{(3)}$	$\mathcal{A}^{(4)}$	$\mathcal{A}^{(5)}$
$\mathcal{A}^{(1)}$	-14.4	-15.8	1.5	-5.4	10	$\mathcal{A}^{(1)}$	-1.4	-19.2	7.2	-5.5	7.4
$\mathcal{A}^{(2)}$	-13.2	5.8	-8.7	-2.2	-18.2	$\mathcal{A}^{(2)}$	-18.5	-20.0	-14.4	-17.6	-5.1
$\mathcal{A}^{(3)}$	-5.9	-19.0	-0.7	-2.0	-19.5	$\mathcal{A}^{(3)}$	3.6	5.5	10	-13.3	-4.9
$\mathcal{A}^{(4)}$	0.8	4.7	-14.8	2.5	-4.1	$\mathcal{A}^{(4)}$	9.8	-12.3	0.6	-16.5	-13.0
$\mathcal{A}^{(5)}$	-11.3	-8.2	-20.0	-17.3	-17.6	$\mathcal{A}^{(5)}$	-11.8	-20.0	-2.4	7.1	-2.3

Matrix 9						Matrix 10					
$a_2 \backslash a_1$	$\mathcal{A}^{(1)}$	$\mathcal{A}^{(2)}$	$\mathcal{A}^{(3)}$	$\mathcal{A}^{(4)}$	$\mathcal{A}^{(5)}$	$a_2 \backslash a_1$	$\mathcal{A}^{(1)}$	$\mathcal{A}^{(2)}$	$\mathcal{A}^{(3)}$	$\mathcal{A}^{(4)}$	$\mathcal{A}^{(5)}$
$\mathcal{A}^{(1)}$	-4.5	-5.2	-8.4	-8.9	5.5	$\mathcal{A}^{(1)}$	-8.4	-1.8	-20.0	7.3	-3.0
$\mathcal{A}^{(2)}$	-12.4	-9.5	8.8	5.4	4.4	$\mathcal{A}^{(2)}$	-8.7	1.7	4.8	2.0	-7.8
$\mathcal{A}^{(3)}$	-4.6	1.3	5.5	7.3	-6.8	$\mathcal{A}^{(3)}$	-13.3	-3.2	0.7	-1.8	-10.7
$\mathcal{A}^{(4)}$	9.0	-18.7	-18.2	-13.7	-8.2	$\mathcal{A}^{(4)}$	9.8	-12.3	0.6	-16.5	-13.0
$\mathcal{A}^{(5)}$	2.2	-9.1	10	7.1	-20.0	$\mathcal{A}^{(5)}$	1.8	2.9	-1.1	10	8.2

B.2 StarCraft II Micromanagement (SMAC) Tasks

B.2.1 Benchmarking on StarCraft II Micromanagement Tasks

In section 5.2, we have compared and discussed the advantage of our approach against baselines on several representative maps. Here we further compare our reproach against baselines on all maps. The SMAC benchmark contains 14 maps that have been classified as easy, hard, and super hard. In

this paper, we design one more map 3h_vs_1b1z3h, whose difficulty is comparable with official super hard maps.

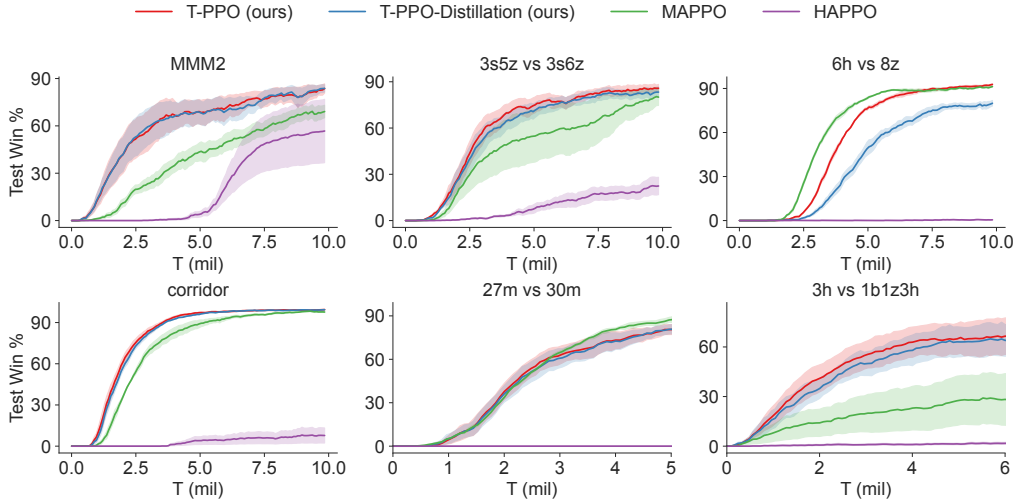


Figure 7: Comparisons between Our approach and policy-based baselines on all **superhard** maps.

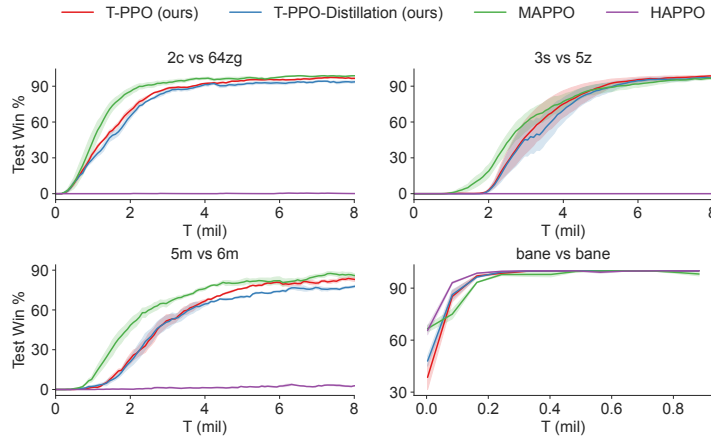


Figure 8: Comparisons between Our approach and policy-based baselines on all **hard** maps.

In Figure. 7, we compare the performance of our approach with baseline algorithms on all super hard maps. We can see that T-PPO outperforms all the baselines, especially on 3s5z_vs_3s6z, MMM2, and 3h_vs_1b1z3h. These results demonstrate that T-PPO can handle challenging tasks more efficiently with theoretical guarantees of its sequential transformation framework, in line with our expectations of it. Meanwhile, our distilled policy T-PPO-Distillation performs similarly to T-PPO, illustrating the competitiveness of our approach to fully decentralized evaluation. HAPPO performs poorly on 4 out of 6 super hard maps, demonstrating its limitation on complex tasks.

Our approach maintains its out-performance on most hard and easy maps. Compared with MAPPO, our approach achieves better convergence points on 3s_vs_5z and 1c3s5z, which confirms the experiment results and analysis in Section 5.1. In summary, T-PPO establishes a new state of the art on SMAC benchmark by outperforming all policy-based baselines in 11 out of 15 scenarios. Meanwhile, the distilled strategy of T-PPO performs as well as the original strategy, which maintains a fairer comparison with baselines on fully decentralized execution.

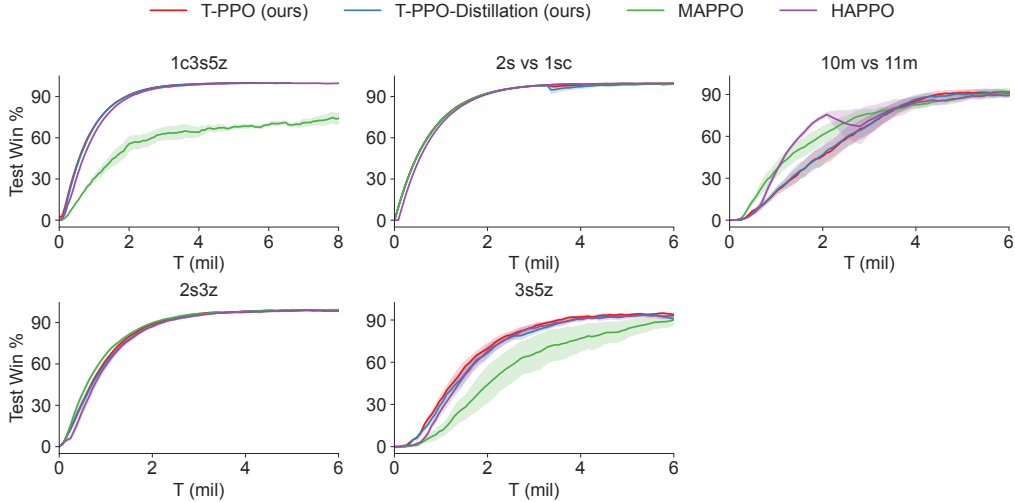


Figure 9: Comparisons between Our approach and policy-based baselines on all **easy** maps.

B.2.2 Hyper-parameters

Our code is implemented based on MAPPO (<https://github.com/marlbenchmark/on-policy>). We share the same structure with MAPPO except improvement we mentioned in Section 4.3 to instantiate our transformation framework. Meanwhile, we share the same hyper-parameters with MAPPO [Yu et al., 2021] only except: (1) We fine-tune the weight of entropy on three maps (0.03 on 3h_vs_1b1z3h, 6h_vs_8z, and 5m_vs_6m) for both our approach and MAPPO. (2) The hyper-parameters of multi-head attention (MHA) modules. As for HAPPO, we use the officially released code and related hyper-parameters (<https://github.com/cyanrain7/TRPO-in-MARL>).

Table 8: Common hyper-parameters for our approach in the SMAC domain.

common hyperparameters	value
MHA heads	3
MHA latent dimension	4
MHA norm weight	0.001
entropy weight	0.01

B.2.3 Distillation

The distillation is just independent behavioral cloning for each agent.

Denote the joint policy as $\pi_{jt}(\cdot|s)$, and the decentralized policy for agent i as $\pi_{\text{deccen}}^i(\cdot|s; \theta)$. The independent behavioral cloning is equivalent to minimization of the KL divergence between the joint policy $\pi_{jt}(\cdot|s)$ and the joint decentralized policy $\prod_{i=1}^n \pi_{\text{deccen}}^i(\cdot|s; \theta)$.

$$\begin{aligned}
& \text{KL} \left(\pi_{jt}(\cdot|s) \left\| \prod_{i=1}^n \pi_{\text{deccen}}^i(\cdot|s; \theta) \right. \right) \\
&= \sum_{\mathbf{a}=(a_1, \dots, a_n)} \pi_{jt}(\mathbf{a}|s) \log \frac{\pi_{jt}(\mathbf{a}|s)}{\prod_{i=1}^n \pi_{\text{deccen}}^i(a_i|s; \theta)} \\
&= \underbrace{\mathbb{E}_{\mathbf{a} \sim \pi_{jt}(\cdot|s)} \left[- \sum_{i=1}^n \log \pi_{\text{deccen}}^i(a_i|s; \theta) \right]}_{\text{behavioural cloning loss}} - \underbrace{H(\pi_{jt}(\cdot|s))}_{\text{entropy (a constant)}}
\end{aligned}$$

B.3 Google Research Football (GRF) Tasks

Because there are fewer agents in GRF compared with SMAC (3 in `Academy_3_vs_1_with_Keeper` and 4 in `Academy_Counterattack_Hard`), we slightly decrease the number of MHA heads from 3 to 2 as shown in Table 9. Other hyper-parameters remains the same as SMAC.

Table 9: Common hyper-parameters for our approach in the GRF domain.

common hyperparameters	value
MHA heads	2
MHA latent dimension	4
MHA norm weight	0.001
entropy weight	0.01

B.4 Running time of T-PPO

The sequential update does take longer time than the concurrent update in the training phase, while in the testing phase, our algorithm doesn't take extra time since a decentralized policy is already calculated by distillation.

Specifically, in the training phase, our framework takes n times the time to do action inference, where n is the number of agents. However, it's worth mentioning that, the time of action inference is only part of the time doing a whole training iteration, which also includes environment simulation and policy training. On the whole, the training time cost of our framework is 0.91 times more than MAPPO in SMAC environment 3m (3 agents), and 1.76 times more in SMAC environment 10m vs 11m (10 agents). This result embodies a trade-off between training time and training performance.

Specific time of each part is shown Table 10.

Table 10: Comparison between TPPO and MAPPO on training time

Env: 3m (1M)	Action inference: t_I	Env simulation: t_S	Env interaction: $t_I + t_S$	Policy Training: t_P	The whole training phase: $t_I + t_S + t_P$
T-PPO	1694.6s	915.4s	2610s	233.7s	2843.7s
MAPPO	434.9s	904.5s	1339.4s	151.9s	1491.3s
Ratio	3.9	1.01	1.95	1.54	1.91
Env: 10m vs 11m (1M)	Action inference: t_I	Env simulation: t_S	Env interaction: $t_I + t_S$	Policy Training: t_P	The whole training phase: $t_I + t_S + t_P$
T-PPO	5011.7s	2065.5s	7077.2s	794.1s	7871.1s
MAPPO	501.1s	2063.2s	2564.3s	292.1s	2856.4s
Ratio	10.0	1.0	2.76	2.72	2.76

B.5 Comparison between T-PPO and other Actor-Critic baselines

We also compare T-PPO with two more actor-critic methods – DOP and FOP on three superhard SMAC maps for completeness. The result is shown in Figure 10.

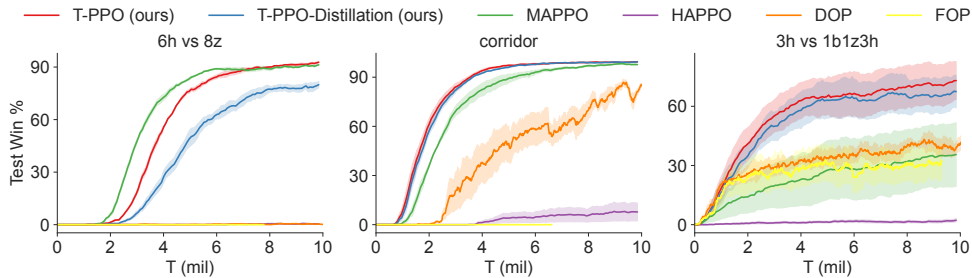


Figure 10: Comparisons between T-PPO and other on-policy baselines on three **superhard** maps.

B.6 T-DQN results

We also implement the off-policy method T-DQN based on the single agent algorithm DQN [Mnih et al., 2013] for completeness. In Figure 11 We evaluate DQN on a Markov Game (Matrix games with random transition), a **hard** and a **superhard** SMAC maps to show that our framework is also compatible with off-policy methods.

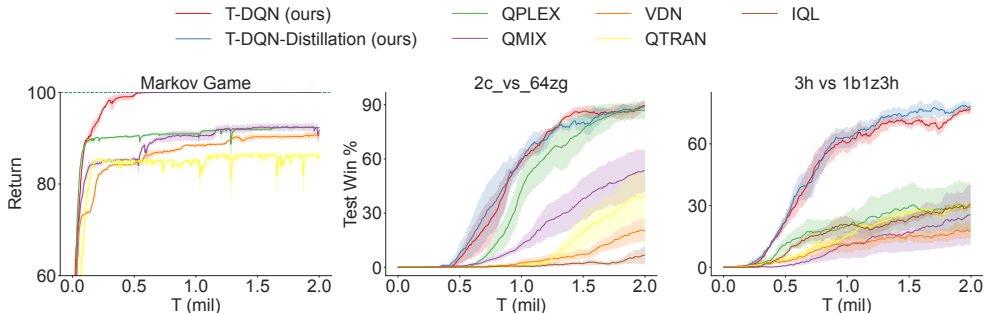


Figure 11: Comparisons between T-DQN and off-policy baselines on Markov Game, a **hard** and a **superhard** SMAC maps.

B.7 Learned behaviour of the sequential framework

We visualize the policy learned by our approach and compare it with MAPPO in MMM2. Based on the comparison, we notice an interesting phenomenon. The joint strategy trained by MAPPO is usually conservative, only moving in a small area, and only two agents are left in the end. On the contrary, the joint strategy trained by our approach is more aggressive. Our agents pull back and forth frequently based on opponents’ movement in a large-scale range while ensuring effective fire focus. We think this phenomenon is caused by our sequential transformation framework, which enables each agent to fully understand the team strategy for more efficient coordination.